

# Semi-classical Over Barrier Model for low-velocity ion-atom charge exchange processes

Fabio Sattin\*

*Consorzio RFX, Associazione Euratom-ENEA ,  
Corso Stati Uniti 4, 35127 Padova, Italy*

(Dated: October 26, 2018)

## Abstract

We develop an Over Barrier Model for computing charge exchange between ions and one-active-electron atoms at low impact energies. The main feature of the model is the treatment of the barrier crossing process by the electron within a simplified quantum mechanical formulation which takes into account: (a) the probability of electron reflection even for over-barrier scattering, and (b) the discreteness of the receiving atom's quantum levels which strongly suppress captures far from the resonance condition. It is shown that inclusion of these effects yields a fairly good prediction of experimental data. We discuss also the probability of electron re-capture by the target.

PACS numbers: 34.70+e, 34.10.+x

---

\*Electronic address: [sattin@igi.pd.cnr.it](mailto:sattin@igi.pd.cnr.it)

## I. INTRODUCTION

Charge exchange processes between slow atomic particles are of great importance in plasma physics and astrophysics. By “slow” we mean that the interparticle velocity is smaller than the classical velocity of the exchanged electron.

While only quantum mechanical (QM) methods can give really accurate computations of all of the basic quantities for these processes, i.e. total and partial or differential cross sections, less precise but simpler methods can still be highly valuable when only moderate accuracy is sought. In the medium-to-high impact velocity range most preferences go to the Classical Trajectory Monte carlo (CTMC) method, which is also more and more often successfully applied also to the low velocity range (see e.g. [1, 2] for a discussion and some recent improvements on this subject). However, the CTMC method has two disadvantages: (i) it is entirely numerical in character, thus somewhat masking the underlying physics; (ii) it relies on large numbers of simulations, thus being rather time-consuming. For these reasons, analytical or semi-analytical methods can still be useful. Over barrier models (OBM) are an example of these models. They are known since a long time [3] and are still being improved to include as much physics as possible [4, 5, 6, 7, 8].

In this work we present a new version of the OBM. It is based upon the papers [5, 7, 8], but is more than a simple refinement: we adopt here the approach of [6], assuming that it is always possible to improve any classical model by turning to a mixed description where some terms are computed using quantum mechanics. The main defect of model [5] is that it very often predicts too large a capture probability. To cure it, we were forced in works [7, 8] to artificially reduce the capture probability by arbitrarily reducing the capture region. We show here that similar results can be achieved in a more self-consistent way if the potential–barrier–crossing process by the electron is described as a quantum mechanical process. In particular, two typical QM features are taken into account: (i) the fraction of electrons crossing the barrier from the target atom to the projectile, which classically is a term of exclusively geometrical origin, must be corrected by a factor  $f_t < 1$ , accounting for the fact that a flux of quantal objects impinging on a potential hill suffers partial reflection even if their kinetic energy is larger than the hill’s height. (ii) Furthermore, within the classical picture the flux of electrons to the projectile is a continuous stream while, quantum–mechanically, it is a resonant process, occurring only when the conditions are satisfied for

which the electron binds to a quantized energy level. We try to implement this feature by adding a modulation term,  $w$ , to the capture probability, near zero far from the resonance condition.

It is important to notice that, although QM corrections are empirically added to find convergence with experiments and/or other computations, no fitting parameters are added: instead, any new parameter needed is estimated on the basis of (semi)quantitative reasoning: once we accept the classical–quantal mixed description, the model is entirely self-consistent. Another important point to stress is that our goal is to merge the QM treatment within the classical one without burdening too much the resulting computations. We shall show that through a drastical simplification of the QM computations we are able to have at the same time rather accurate results written in terms of simple formulas.

Finally, we try to implement in a consistent fashion within the model the possibility by the target of re-capturing the electron once it has been bound to the projectile. The importance of this effect on the effective capture efficiency, and the limitations of the approach adopted, will be briefly discussed in the appendix.

## II. DESCRIPTION OF THE OBM

We consider a scattering experiment between a nucleus  $\mathbf{T}$  with an active electron  $\mathbf{e}$ , and a projectile nucleus  $\mathbf{P}$ . Let  $\mathbf{r}$  be the electron position relative to  $\mathbf{T}$  and  $\mathbf{R}$  the relative distance between  $\mathbf{T}$  and  $\mathbf{P}$ . Let us further consider all the three particles lying within the same plane  $\mathcal{P}$ . We label the direction along the internuclear axis as the  $z$  axis and describe the position of the electron using cylindrical coordinates  $(\rho, z, \phi \equiv 0)$ . The two nuclei are considered as approaching at a velocity very small if compared to the orbital electron velocity. The total energy of the electron is

$$E(R) = \frac{p^2}{2} + U(z, \rho, R) = \frac{p^2}{2} - \frac{Z_t}{\sqrt{\rho^2 + z^2}} - \frac{Z_p}{\sqrt{\rho^2 + (R - z)^2}} \quad . \quad (1)$$

where  $Z_p$  and  $Z_t$  are the effective charge of the projectile and of the target seen by the electron, respectively (we are considering hydrogenlike approximations for both the target and the projectile). Atomic units are used unless otherwise stated. Notice that our reference frame is non inertial, so other terms as Coriolis and centrifugal force should arise. We discard them on the basis of the low-velocity approximation.

As long as the electron is bound to **T** we can approximate  $E$  by

$$E(R) \doteq -E_n - \frac{Z_p}{R} \quad (2)$$

with  $E_n > 0$  the unperturbed binding energy of the electron to **T**.

On the plane  $\mathcal{P}$  we can draw a section of the equipotential surface

$$U(z, \rho, R) = E(R) = -E_n - \frac{Z_p}{R} \quad . \quad (3)$$

The set of points  $(\rho, z)$  that satisfy this equation mark the limits of the region classically allowed to the electron. When  $R \rightarrow \infty$  this region is disconnected into two circles centered around each of the two nuclei. As  $R$  diminishes the two regions can eventually merge. It is the opening of the equipotential curve between **T** and **P** which leads to a leakage of electrons from one nucleus to another, and therefore to charge exchange. It is possible to solve Eq. (3) in the limit of vanishing width of the opening ( $\rho \equiv 0$ ), and find:

$$R_m = \frac{(\sqrt{Z_t} + \sqrt{Z_p})^2 - Z_p}{E_n} \quad . \quad (4)$$

In the region of the opening the potential has a saddle structure: along the internuclear axis it has a maximum at

$$z = z_0 = R \frac{\sqrt{Z_t}}{\sqrt{Z_p} + \sqrt{Z_t}} \quad (5)$$

In our work, following [5], we assume that the electron is in a low angular momentum state (e.g. an  $s$  states), thus unperturbed classical electron trajectories can be visualized as straight segments in the radial direction, starting from the target nucleus. We assume also that the qualitative shape of the trajectory is not changed by the collision: the electron free falls towards **P**.

Charge loss occurs provided that the electron is able to cross the potential barrier. Let  $W$  be the probability for the electron to be still bound to **T** at time  $t$ . We write its rate of change as

$$\frac{dW(t)}{dt} = -N_t \frac{1}{T_t} f_t W(t) \quad (6)$$

Notice that we have defined the probability for an electron to be bound at **P** as  $1 - W(t)$ , thus ruling out the possibility of ionization, which is, however, small for low-energy collisions.

Let us now explain the meaning of the terms in the right hand side of this equation: we identify  $N_t$  as the fraction of classical particles which at time  $t$  leave the target as a consequence of their motion. It is simply a geometrical factor: assuming a uniform distribution of electron trajectories, it is equal to the ratio between the solid angle intercepting the opening and the total  $4\pi$  solid angle. The azimuthal integration is straightforward and thus

$$N_t = \frac{1}{2} \left( 1 - \frac{z_0}{\sqrt{z_0^2 + \rho_m^2}} \right) \quad (7)$$

with  $\rho_m$  half-length of the opening in the radial direction, root of

$$E_n + \frac{Z_p}{R} = \frac{Z_t}{\sqrt{z_0^2 + \rho_m^2}} + \frac{Z_p}{\sqrt{(R - z_0)^2 + \rho_m^2}} \quad (8)$$

A useful approximation is to expand Eq. (8) and then Eq. (7) in powers of  $\rho_m/R$  and retain only terms up to the second order. This was justified in the original paper [5] by the need of accurately modelling far collisions. However, this approximation turned out to be a rather accurate one since close encounters are weighted in the final cross section by the (small) impact parameter, thus even a rough estimate is not so much important.

With this approximation, the calculation is straightforward and we find

$$N_t = \frac{1}{2} \frac{\sqrt{Z_p/Z_t}}{(\sqrt{Z_p} + \sqrt{Z_t})^2} \left[ (\sqrt{Z_p} + \sqrt{Z_t})^2 - Z_p - E_n R \right] \quad (9)$$

The parameter  $T_t$  is the classical period of the electron bound to  $\mathbf{T}$ . It accounts for the fact that if the classical phases within the ensemble of the electrons are randomly distributed, during the time interval  $dt$  only the fraction  $dt/T_t$  come through the opening. The period can be calculated using the semiclassical relation  $T_t = 2\pi n_{\text{eff}}^3$  (see e.g. [7]) with  $n_{\text{eff}}$  an effective quantum number for the electron bound to  $\mathbf{T}$ , which can be computed from eq. (2) through  $E_n = Z_t^2/(2n_{\text{eff}}^2)$ . The result is

$$T_t = 2\pi \left( \frac{Z_t^2}{2E_n} \right)^{3/2} \frac{1}{\left( 1 + \frac{Z_p}{E_n R} \right)^{3/2}} \quad (10)$$

The factor  $T_t^0 = 2\pi(Z_t^2/(2E_n))^{3/2}$  is the unperturbed period. It is clear from eq. (10) that  $T_t/T_t^0 < 1$ , and it was shown in [8] that the average (or effective) value of this ratio is typically of the order of 0.5.

Finally,  $f_t$  accounts for quantum mechanical corrections to the barrier crossing probability.

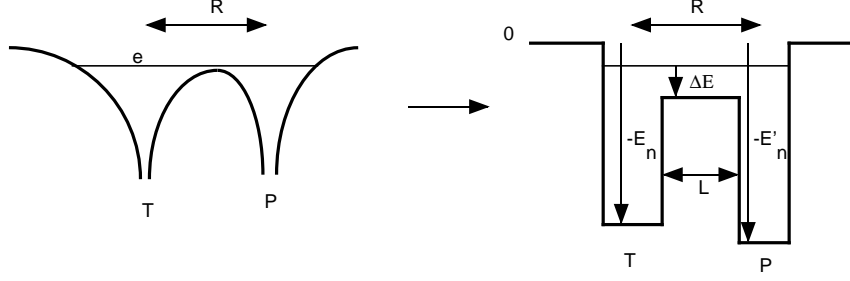


FIG. 1: Pictorial view of the potential along the internuclear axis as it is (left figure) and how it is approximated by the rectangular square approximation (right figure).

Classically  $f_t \equiv 1$ , while a flux of quantum mechanical particles impinging on a potential barrier is reduced by a factor  $f_t < 1$  even though the kinetic energy of the particles is larger than the height of the hill. In order to reduce computation of  $f_t$  to an easily manageable form we must replace the true potential profile with a model barrier whose transmission factor can be analytically computed. The choice of the model potential can be crucial for final results, so we have tested two candidates. The former choice is the rectangular barrier; in fig. (1) we draw a schematic picture of the potential profile along the internuclear axis: as it is (left-hand figure), and as it is approximated (right-hand figure). The horizontal line labelled by “e” marks the energy of the electron. The zero of the potential well associated at the target is chosen so that the binding energy of the electron is equal to its unperturbed value  $E_n$ , and analogously  $E'_{n'}$  is the binding energy to the projectile (till now undefined). The potential barrier between the two nuclei is depressed so that the electron is able to cross it with a kinetic energy  $\Delta E$ . The width of the potential barrier is set to  $L$ , yet undefined but of the order of the internuclear distance  $R$ . The transmission factor TF for an electron coming from the left of the potential hill is

$$\text{TF} = \frac{e^{-\frac{i}{2}L(k-2q+s)} 4kq}{k [(q+s) + e^{2iLq} (q-s)] + q [(q+s) - e^{2iLq} (q-s)]} \quad (11)$$

with  $k = \sqrt{2E_n}$ ,  $q = \sqrt{2\Delta E}$ ,  $s = \sqrt{2E'_{n'}}$  electron momenta respectively in the **T** potential well, in the potential barrier, and in the **P** potential barrier. Of course, the relation holds

$$f_t = |\text{TF}|^2 \quad . \quad (12)$$

The binding energy to the projectile can be calculated by considering that, when **e** is bound to **P**, its energy is  $E(R) = -E'_{n'} - Z_t/R$ , with  $E'_{n'} = Z_p^2/(n')^2$ . At the capture radius this

expression and that given by eq. (2) must be equal, thus

$$E'_{n'} = E_n + \frac{Z_p - Z_t}{R} \quad . \quad (13)$$

We compute  $q$  along the internuclear axis: by using eqns. (1,2,5), it is quite easy to work out

$$q = k \left( \frac{R_m}{R} - 1 \right)^{1/2} \quad . \quad (14)$$

It remains to estimate  $L$ . Of course, given the way eq. (11) has been derived, only a semi-quantitative estimate is required. By a straightforward application of the virial theorem, one finds

$$\left\langle \frac{p^2}{2} \right\rangle \doteq \frac{1}{2} Z_t \left\langle \frac{1}{S_t} \right\rangle \approx \frac{1}{2} \frac{Z_t}{\langle S_t \rangle} \quad (15)$$

and

$$\left\langle \frac{p^2}{2} \right\rangle - Z_t \left\langle \frac{1}{S_t} \right\rangle = -E_n \quad (16)$$

with  $2 \langle S_t \rangle$  average width of the potential well. A similar relation holds for the potential well centered around the projectile. From the two previous equations we find  $\langle S_t \rangle = 1/2(Z_t/E_n)$ ,  $\langle S_p \rangle = 1/2(Z_p/E'_n)$ , thus,

$$L = R - (\langle S_t \rangle + \langle S_p \rangle) = R - \frac{Z_t}{2E_n} - \frac{Z_p}{2E'_n} \quad . \quad (17)$$

Of course, we set  $L = 0$  when the right-hand side of the equation above is lesser than zero. By taking a glance at eqns. (11,17), one can guess that the effective number of captures  $f_T N_T$  is strongly suppressed already for  $R < R_m$ : this is exactly what found in CTMC simulations (see [7]). In order to take an insight at what the transmission factor looks like, we plot in fig. (2)  $f_t$  given by Eq. (11) for H - H<sup>+</sup> scattering. In the same way as the laws of quantum mechanics prevent a fraction of electron to be captured even when it would be classically allowed, they also—through tunnelling—would make it possible for some electrons to be captured even at internuclear distances  $R > R_m$ . However, it is easy to show that this correction to the total capture probability is very small, and thus we will neglect it.

This model potential is extremely useful for calculations but one could wonder if it is too drastic an approximation, particularly in view of the fact that it is not smooth. As a test, we have replaced the rectangular barrier with an Eckart potential [9]

$$V(x) = 4V_0 \frac{e^{\frac{x}{\lambda}}}{(1 + e^{\frac{x}{\lambda}})^2} \quad , \quad (18)$$

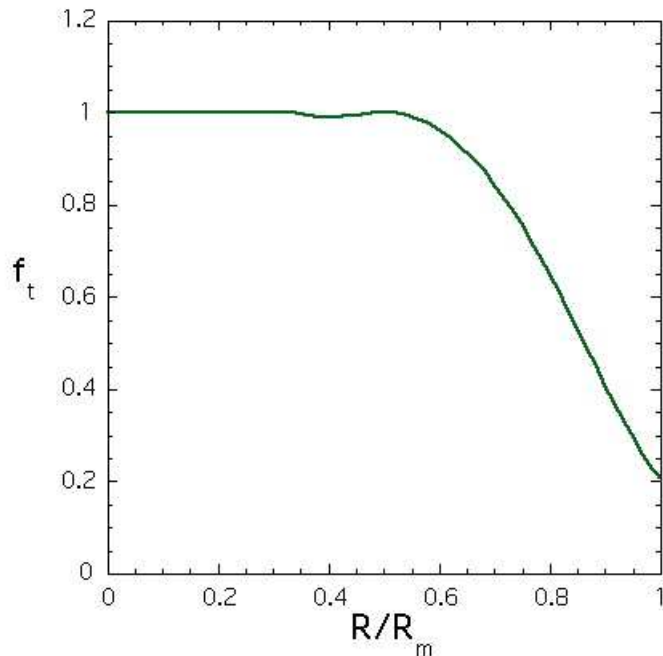


FIG. 2: Transmission factor  $f_t$  (Eq. 11) for H - H<sup>+</sup> collisions. Notice that the probability of transmission falls well below one already for values of  $R$  rather far from the maximum allowed capture distance  $R_m$  (Eq. 4).

which is instead a smooth, bell-shaped curve (see fig 3). The transmission factor for this potential is analytically computable and, for a particle of momentum  $p$ :

$$f_t = \frac{\cosh(4\pi p\lambda) - 1}{\cosh(4\pi p\lambda) + \cosh(4\pi\sqrt{2\lambda^2 V_0 - 1/16})} \quad . \quad (19)$$

The parameters  $\lambda, V_0, p$  can be straightforwardly related to the parameters  $L, k, q, s$  given above. The quantity  $f_t$  in (19) is a mildly varying function of  $\lambda$  but is, unfortunately, a strong function of  $E/V_0$ , going steeply from zero to one as this ratio crosses the unity. This is a deprecable feature since, as it appears clear from the equations (13-17) above, we can give only semiquantitative estimates-therefore likely to have a large variability-for all the quantities involved.

A main difference between the classical picture and the quantum-mechanical one is that the former depicts the capture process as a continuous flow. On the contrary, quantization

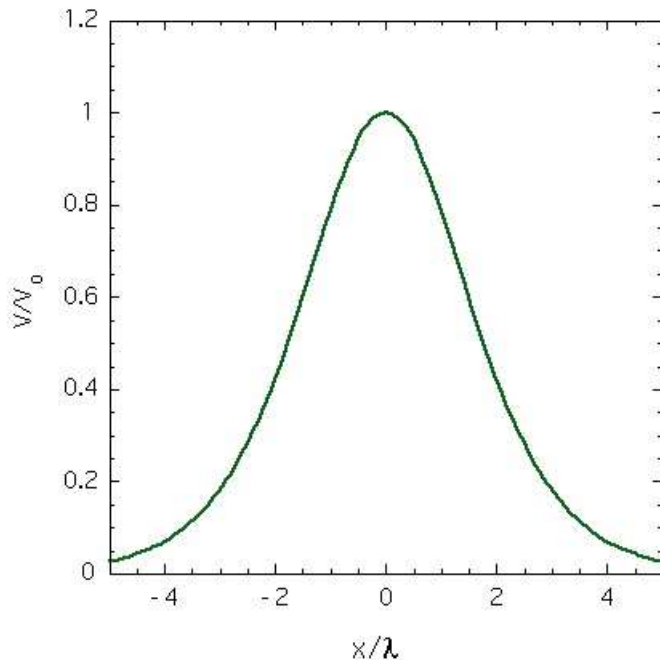


FIG. 3: Eckart potential (Eq. 18).

rules forbid the electronic flow from one nucleus to the other unless some resonance conditions are satisfied: by using the relation (13), we obtain

$$R(n') = \frac{Z_p - Z_t}{\frac{1}{2} \frac{Z_p^2}{(n')^2} - E_n} \quad , \quad (20)$$

that is, captures should be allowed only close to these values of  $R$ , in correspondence of integer values  $n'$ .

In this work we want to implement an algorithm to take into account the damping of capture probability far from these resonances, persuaded that this should drastically improve the predictions of the model.

We choose to implement phenomenologically this feature by modulating  $f_t$  with a weight function  $w$  centered around the values  $R(n')$ . For  $w$  we choose a sum of Gaussians

$$w(R) = \sum_{n'} \exp \left[ - \left( \frac{R - R(n')}{\Delta R(n')/2} \right)^2 \right] \quad . \quad (21)$$

It is necessary to find a reasonable value for  $\Delta R(n')$ . For this we resort to the indeterminacy relations: infact,  $\Delta R \rightarrow 0$  means that the energetic levels for the projectile are sharply

defined, while any finite value for  $\Delta R$  means that they are defined only within an energy range  $\Delta E$ . We suppose that the usual indeterminacy relations hold:  $\Delta E \times \Delta t \doteq 1/2$ . Within the straight-line trajectory approximation,  $\Delta t \approx \Delta R/u$  while, using again Eq. (13) and differentiating with respect to  $R$ , we get  $\Delta E \approx (Z_p - Z_t)/R^2 \Delta R$ . Collecting the above expressions,

$$\Delta R(n') \approx \sqrt{\frac{1}{2} \frac{u R^2(n')}{Z_p - Z_t}} . \quad (22)$$

The above expression breaks down when  $Z_p = Z_t$ . In that case we will not adopt this approach, instead we will assume uniform probability of capture all along the internuclear distance:  $w \equiv 1$ . Notice that, with the above definitions, it seems that we get as a bonus also partial probabilities for capture into well defined quantum numbers: if we are interested in captures into state  $m$ , it is enough to truncate the sum  $w$  (Eq. 21) to the single term corresponding to  $n' = m$ . As we shall see later, this picture however does not hold.

Eq. (6) can be formally integrated till the end of collision:

$$W(t = \infty) = \exp \left[ - \int_{-\infty}^{\infty} \left( \frac{w f_t N_t}{T_t} \right) dt \right] . \quad (23)$$

The capture probability is  $P = 1 - W(\infty)$ . We assume a straight-line trajectory for the projectile:  $R = \sqrt{b^2 + (ut)^2}$ , with  $b$  impact parameter and  $u$  its velocity. Total charge exchange cross section is thus

$$\sigma = 2\pi \int b P db . \quad (24)$$

Equation (23) cannot be analytically integrated unless we make further simplifications. However, it is quite easily numerically integrated by any standard mathematical software package.

### III. RESULTS

We will benchmark the model against the experimental results from ref. [10] and the theoretical ones coming from the molecular approach simulation of ref. [11]. In fig. (4) we show the results for impact between multicharged hydrogenlike ions and ground state hydrogen. In all case impact velocity is about 1/2 (it is rigorously so for numerical results, while in experiments  $0.49 \leq u \leq 0.51$ ). Meyer et al. [10] published also results from other non-hydrogenlike ions, with the same charge states; since, for a given charge, cross sections

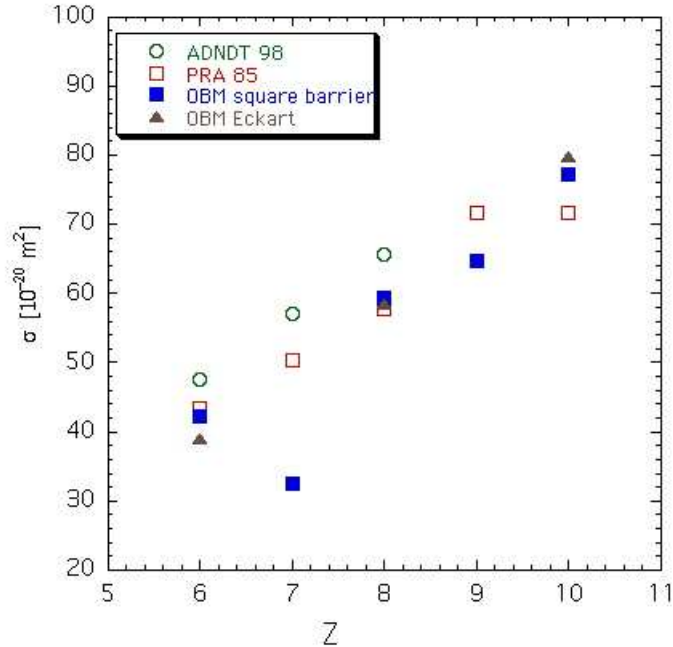


FIG. 4: Charge exchange cross section versus projectile charge. Open circles, data from ref. [11]; open squares, data from ref. [10]; full squares, OBM results using rectangular barrier potential; triangles, OBM results using Eckart potential (Eq. 18).

are not qualitatively different, we have limited to the present selection and got rid of the complications involved with the definition of effective charges.

Let us now discuss the results of fig. (4). The OBM with the choice of the rectangular barrier as model potential (black squares) fairly well overlaps experimental data for all cases but  $N^{7+}$ . The reason lies in a combination of effects, which we will discuss below. Let us comment instead, the results from the other simulation (black triangles): they have been computed using Eckart potential (Eq. 18). Even if at first sight these results look pretty accurate, things are not that good. Actually, in order to reach this accuracy, we have had to increase the barrier height  $V_0$  so as to allow only grazing incidence,  $E = V_0$  (or  $q \approx 0$ , using notations of rectangular barrier potential). This, since Eckart potential has a strong transmission factor for  $E/V_0$  even slightly larger than one. Using the same conditions as for the rectangular barrier would yield an overestimate of the true cross section.

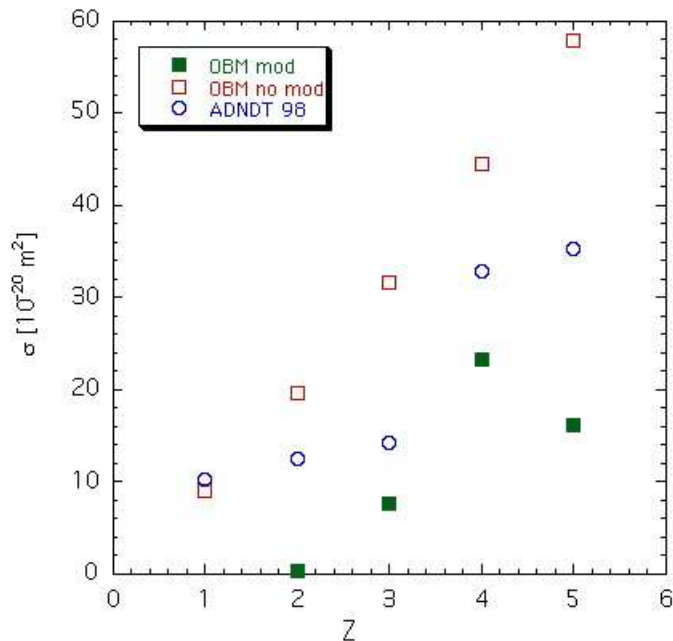


FIG. 5: Charge exchange cross section versus projectile charge,  $1 \leq Z \leq 5$ . Open circles, data from ref. [11]; full squares, OBM results using rectangular barrier potential; open squares, same as full squares but without modulation of the transmission factor.

Let us now consider fig. 5: it is alike fig. 4 but with  $1 \leq Z \leq 5$ . Only data from ref. [11] are available for these ions. In this case we have computes  $\sigma$  using only  $f_t$  from Eq. (12) but with  $w$  given by Eq. (21) (solid circles) or with  $w \equiv 1$  (empty circles). The only exception being hydrogen, for which only  $w = 1$  can be used. It is apparent that some sort of modulation of the transmission factor is needed in order to avoid an overestimate of  $\sigma$ . The effect of the modulation is to underestimate the cross section, but some charge states are more damped than others. It is the same effect, but enhanced, seen in fig. 4. The reason of the failure of the model in these cases lies in a balance between attenuation factors and resonances positions. In order to better visualize it, let us consider fig. 6: there, we have plotted, for ions with charge  $6 \leq Z \leq 9$ , the position of each resonance  $R(n)$  [normalized to the maximum capture distance  $R_m$  given by Eq. (4)] versus the quantum number  $n$ . The bars superposed to the points mark the width of the resonance: they are the  $\Delta R(n)$ 's

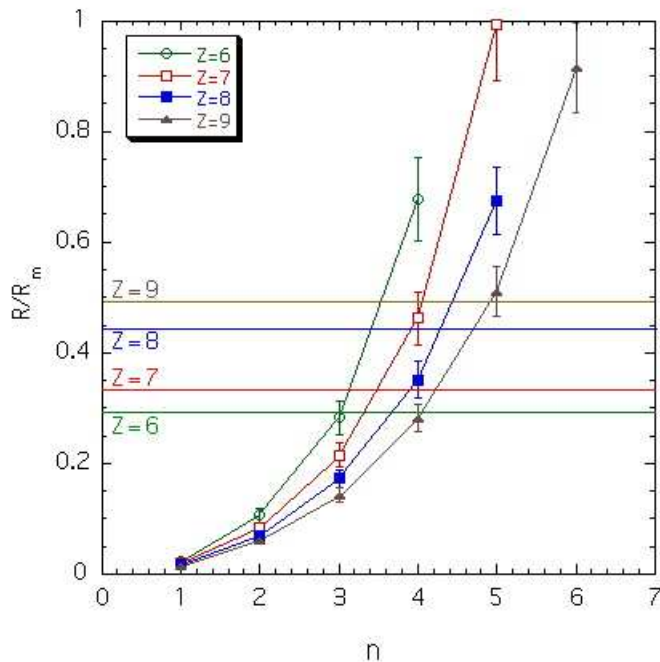


FIG. 6: Normalized capture distance *versus* quantum number, for some highly-charged ions. Horizontal lines mark, for each ion the distance at which the attenuation factor (12) is reduced to one half.

given by Eq. (22). The horizontal lines label the distance at which the capture probability is reduced to 1/2 because of the factor (12). Thus, capture is effective only into quantum numbers whose resonance position lies below this line. We compare, for example, carbon ( $Z = 6$ ) to nitrogen ( $Z = 7$ ): in both cases, attenuation  $f_t$  limits capture effectively to the first three states, and impact parameter considerations lead to suggest that  $n = 3$  is the dominant state. However, the resonance width of  $n = 3$  is lesser for nitrogen than for carbon, thus explaining the reduced capture cross section. Similar considerations, but a lesser extent, hold for  $Z = 8$  and  $Z = 9$ . It is clear that slightly charged ions, for which captures only in few states are possible, are particularly sensitive to this effect. Different is the case for hydrogen, where, as explained in the previous section, no considerations of resonances apply. Notice, however, that oscillations in capture cross sections with the charge, due to discreteness of quantum levels, are not an artifact of the model but, albeit with different features, have

been experimentally observed [3].

#### IV. CONCLUSIONS

In this work we have presented a version of Over Barrier Model for computation of charge exchange cross sections. The model presents some unusual features, such as the inclusion within its classical background of quantum elements. We showed it to be quite reliable in a well defined range of parameters, namely in the low-energy, medium-to-high-projectile charge region, where it presents noticeable improvements with respect to other similar algorithms. The reasons for poorer performances in other parameters space regions have been clearly identified and some insights about possible further improvements are possible: the first candidate to work on to reach an overall fairly good accordance with experiment is the modulation factor  $w$  (Eq. 21); presently, however, we are not able to guess if a general optimal expression is possible, valid for all projectile-target combinations.

#### APPENDIX A

It is straightforward to adapt Eq. (6) to accomodate the possibility for the captured electron to return to the target nucleus: it is enough to add a term

$$\frac{dW(t)}{dt} = -N_t \frac{1}{T_t} f_t W(t) + N_p \frac{1}{T_p} f_p (1 - W(t)) \quad (\text{A1})$$

The second term in the r.h.s. represents the flux of electrons which have previously been captured by **P** and that now cross a second time the barrier in the opposite direction, thus being re-captured by **T**. The definition of the parameters  $N_p, T_p, f_p$  is the same as given in the previous sections, see Eqns . (7,10,12), with the trivial exchange of the projectile with the target.

Eq. (A1) can be solved exactly in terms of quadratures. Here, we will show that it is possible from this equation to recover the result for symmetrical scattering: infact, in this case,  $f_t = f_p$ ,  $N_t = N_p$  and  $T_t = T_p$  and, by setting  $f_t N_t / T_t = f_p N_p / T_p = \varphi$  for brevity, and

$\int_{-\infty}^t \varphi(\tau) d\tau = \Phi(t)$ , we get

$$\begin{aligned}
P &= 1 - e^{-2\Phi(\infty)} \left[ 1 + \int_{-\infty}^{\infty} \varphi(\tau) e^{2\Phi(\tau)} d\tau \right] \\
&= 1 - e^{-2\Phi(\infty)} \left[ 1 + \frac{1}{2} \int_{-\infty}^{\infty} \frac{d}{d\tau} e^{2\Phi(\tau)} d\tau \right] \\
&= 1 - e^{-2\Phi(\infty)} \left[ 1 + \frac{1}{2} (e^{2\Phi(\infty)} - 1) \right] \\
&= \frac{1}{2} [1 - e^{-2\Phi(\infty)}] \quad ,
\end{aligned} \tag{A2}$$

and we recover the prescription for equal-charge scattering.

Of course, we can also recover easily the opposite limit, in which  $Z_p \gg Z_t$ ; in this case we can simply neglect the return term since  $f_p N_p / T_p \ll f_t N_t / T_t$ .

We have verified that the probability of recapture is negligible for all multicharged projectiles. The only exception is the  $Z_p = Z_t$  scattering. However, we found that the use of the symmetrized capture probability (A2) does not improve results in this case, and actually degrades the performances of the model. The reason is that we are overestimating the probability of recapture in Eq. (A1): it holds rigorously in the limit of asymptotically slow nuclear motion,  $u \rightarrow 0$ ; for finite  $u$ , retardation effects should be implemented to take into account that electrons released by the projectile at time  $t$  were captured at an earlier time  $t'$ . However, in the region of velocities where retardation effects can be neglected, other essential features of the model, such as the straight trajectory approximation, break down.

- 
- [1] M.J. Raković, D.R. Schultz, P.C. Stancil and R.K. Janev, J. Phys. A: Math. Gen. **34**, 4753 (2001)
  - [2] D.R. Schultz, P.C. Stancil and M.J. Raković, J. Phys. B: At. Mol. Opt. Phys. **34**, 2739 (2001)
  - [3] H. Ryufuku, K. Sasaki and T. Watanabe, Phys. Rev. A, **21**, 745 (1980)
  - [4] A. Niehaus, J. Phys. B: At. Mol. Phys. **19**, 2925 (1986)
  - [5] V.N. Ostrovsky, J. Phys. B: At. Mol. Opt. Phys. **28**, 3901 (1995)
  - [6] F. Sattin, J. Phys. B: At. Mol. Opt. Phys. **33** 861, 2377 (2000)
  - [7] F. Sattin, Phys. Rev. A **62**, 042711 (2000)
  - [8] F. Sattin, Phys. Rev. A **64**, 034704 (2001)
  - [9] C. Eckart, Phys. Rev. **35**, 1303 (1930)

- [10] F.W. Meyer, A.M. Howald, C.C. Havener and R.A. Phaneuf, Phys. Rev. A **32**, 3310 (1985)
- [11] C. Harel, H. Jouin and B. Pons B, At. Data Nucl. Data Tables **68**, 279 (1998)